

Segregation in aqueous methanol enhanced by cooling and compression

L. Dougan, R. Hargreaves, and S. P. Bates

School of Physics, The University of Edinburgh, Mayfield Road, Edinburgh EH9 3JZ, United Kingdom

J. L. Finney

Department of Physics and Astronomy, University College London, Gower Street, London WC1E 6BT, United Kingdom

V. Réat

Laboratoire "RMN et interactions proteines-membranes," Institut de Pharmacologie et de Biologie Structurale, UMR 5089-CNRS/UPS, 205 Route de Narbonne, 31077 Toulouse Cedex, France

A. K. Soper

ISIS Facility, Rutherford Appleton Laboratory, Chilton, Didcot, Oxon OX11 0QX, United Kingdom

J. Crain

School of Physics, The University of Edinburgh, Mayfield Road, Edinburgh EH9 3JZ, United Kingdom and IBM TJ Watson Research Center, 1101 Kitchawan Road, Yorktown Heights, New York 10598

(Received 30 November 2004; accepted 16 February 2005; published online 5 May 2005)

Molecular segregation in methanol-water mixtures is studied across a wide concentration range as a function of temperature and pressure. Cluster distributions obtained from both neutron diffraction and molecular dynamics simulations point to significantly enhanced segregation as the mixtures are cooled or compressed. This evolution toward greater molecular heterogeneity in the mixture accounts for the observed changes in the water-water radial distribution function and there are indications also of a change in the topology of the water clusters. The observed behavior is consistent with an approach to an upper critical solution point. Such a point would appear to be "hidden" below the freezing line, thereby precluding observation of the two-fluid region. © 2005 American Institute of Physics. [DOI: 10.1063/1.1888405]

I. INTRODUCTION

Amphiphiles are a particularly important class of molecule containing both hydrophobic and hydrophilic domains with competing solubility properties. Association of nonpolar moieties leads to the formation of micelles and other modulated structures. Due to the local density variations inherent to many self-assembled amphiphilic structures, simple equations of state fail to give a complete description of phase equilibria. The simplest amphiphiles (the primary alcohols such as methanol, ethanol and propanol) are widely studied and have been found to be completely miscible in all proportions and at all state points studied. Recently, however, experimental and computational studies on aqueous methanol have revealed unexpectedly complex behavior at medium length scales leading to a substantially revised view of miscibility in this prototype aqueous amphiphile.¹⁻³ In particular, molecular-level segregation has been observed with the alcohol agglomerates exhibiting structural details consistent with those expected for a hydrophobically driven system.^{1,3} Moreover, percolating clusters have been found for both components in a certain concentration range over which many thermodynamic functions and transport properties reach extremal values.⁴

Despite the intense activity and success in studying these model systems at room temperature and pressure, there have been no systematic investigations aimed at mapping out the behavior of these observed extended structures under nonambient conditions. Even in systems which exhibit clear misci-

bility gaps, the pressure dependence of the critical solution temperature can increase, decrease, or remain constant⁵ and little information exists on molecular-level structure. Such measurements on the model methanol-water mixture are needed to develop and refine molecular-level models of the entropic and enthalpic factors governing the phase behavior of aqueous amphiphiles. These models are potentially of wider significance to areas such as membrane and protein stability.

Partial miscibility is a common feature of binary liquid phase equilibria in which a mixture separates into two phases of different compositions⁵ depending on temperature and pressure. This behavior follows directly from the *Gibbs phase rule* and is contained within simple molecular thermodynamic models such as Bragg-Williams theory. Typically, an immiscible region terminates at an *upper critical solution temperature*, above which the mixture is fully miscible. In some hydrogen-bonded systems, however, further cooling leads to reentrant miscibility and a closed-loop gap in the phase diagram appears.⁶⁻⁸ We therefore report here an attempt to explore structural properties of methanol-water mixtures far from the ambient state point. We use a combination of neutron diffraction with comprehensive isotope substitution and classical molecular dynamics simulations. The specific objective of the work is to identify the separate effects of temperature and pressure on the structures formed in these solutions, the combined effects of temperature and pressure

TABLE I. Parameters of the methanol-water mixtures used in the empirical potential structural refinement.

Mole fraction x	Temperature (K)	Pressure (kbar)	Total no. of molecules	No. of methanol molecules	No. of water molecules	No. density (atoms/Å ³)	Box size (Å)
0.27	293	amb	600	162	438	0.0967	28.69
0.27	238	amb	600	162	438	0.0967	28.69
0.50	200	amb	600	300	300	0.1026	29.74
0.50	200	2.0	600	300	300	0.1158	28.57
0.54	298	amb	600	324	276	0.0955	30.52
0.54	260	amb	600	324	276	0.0975	30.26
0.54	190	amb	600	324	276	0.1000	30.73
0.70	293	amb	600	420	180	0.0930	32.04

and to comment on the nature of intermolecular contacts in these solutions.

II. EXPERIMENTAL AND SIMULATION DETAILS

Protiated and deuteriated samples of methanol and water were obtained from Sigma-Aldrich and used without additional purification. Neutron diffraction measurements were performed on the SANDALS time-of-flight diffractometer at the ISIS pulsed neutron facility at the Rutherford Appleton Laboratory in the UK. The liquid samples were contained in flat plate cells constructed from a Ti-Zr alloy from which coherent scattering is negligible. These were mounted on a closed cycle refrigerator, and neutron diffraction measurements were made at a number of different temperatures and pressures (Table I). For the high pressure experiments, the sample was contained in several 1.5 mm cylindrical channels cut into a flat TiZr plate. Pressure was applied using an intensifier. The high pressure experimental arrangement has been described in detail in a previous publication.⁹ The data were corrected for attenuation, inelastic, and multiple scattering using the ATLAS programme suite.¹⁰ The differential scattering cross section for each sample was obtained by normalizing to a vanadium standard sample. A total of seven isotopically distinct samples were measured for methanol mole fractions $x=0.27$, $x=0.54$, and $x=0.70$. These were, respectively, (i) CD₃OD in D₂O, (ii) CD₃OH in H₂O, (iii) a 50:50 mixture of (i) and (ii); (iv) CH₃OD in D₂O; (v) a 50:50 mixture of (i) and (iv); (vi) CH₃OH in H₂O; and (vii) a 50:50 mixture of (i) and (vi). For $x=0.05$, five samples were measured, namely, (i), (ii), (iii), (vi), and (vii) and for $x=0.50$, (i), (ii), (iii), (iv), and (v). These procedures lead to a structure factor $F(Q)$ having the form $F[S_{HH}(Q), S_{XH}(Q), S_{XX}(Q)]$ where $S_{HH}(Q)$ relates to correlations between labeled atoms and $S_{XH}(Q)$ and $S_{XX}(Q)$ are the two composite partial structure factors which give the remaining correlations between other types of atoms (X) and the labeled atom type (H) in the form of a weighted sum of individual site-site partial structure factors.

Diffraction data is analyzed using the empirical potential structure refinement (EPSR) procedure.¹¹ According to this method, a three-dimensional computer model of the solution is constructed and equilibrated using interaction potentials taken from the literature. The charges and Lennard-Jones constants from the SPC/E potential of Berendsen *et al.*¹² were used for the water molecules. The $H1$ potential of

Haughney *et al.*¹³ was used for the methanol molecules. Methanol-water interactions were simulated by Lorentz–Berthelot mixing rules.¹⁴ Information from the diffraction data is then introduced as a constraint whereby the difference between observed and calculated partial structure factors enters as a potential of mean force to drive the computer model (via Monte Carlo updates of atomic positions) toward agreement with the measured data. This procedure results in an ensemble of three-dimensional molecular configurations of the mixture exhibiting average structural correlations that are consistent with the available diffraction data. A total of 600 molecules (methanol and water) are contained in a cubic box of the appropriate dimension to give the measured density of each solution at the appropriate temperature (Table I). Periodic boundary conditions are imposed. A comparison between the experimentally measured partial structure factors and those generated from the ensemble-averaged EPSR with 10 000 configurations is shown in Fig. 1.

We have performed a series of classical molecular dynamics simulations using the DL_POLY code¹⁵ employing previously tested intermolecular potentials for both methanol¹⁶ and water.¹⁷ Both molecular species are modeled using a fully flexible, all-atom approach with specific van der Waals

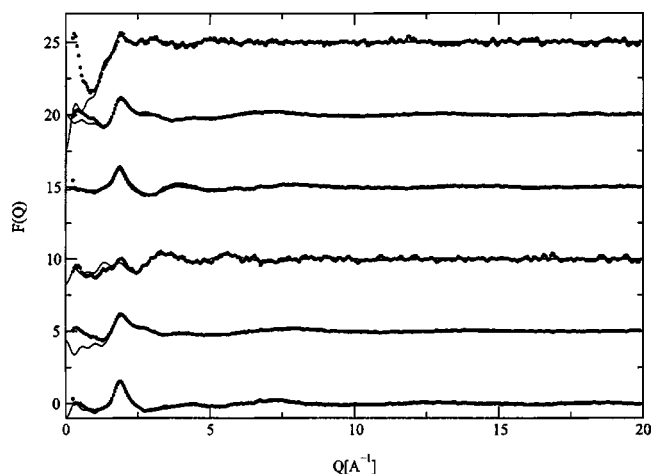


FIG. 1. Typical example of the fits (lines) obtained by the EPSR analysis compared to the original data (circles). The data shown in this case ($x=0.50$ at 200 K and 2 kbar) are the interference differential scattering cross sections for the samples (i)–(vi) described under Methods. Discrepancies are observed in the low Q region. These are caused by difficulties in removing completely the effect of nuclear recoil from the measured data. However this recoil effect is expected to have only a monotonic dependence on Q and so is unlikely to influence the model structure to any significant extent.

TABLE II. Parameters of the methanol-water mixtures used in the molecular dynamics simulations using DL_POLY.

Mole fraction x	Temperature (K)	Pressure (kbar)	Total no. of molecules	No. of methanol molecules	No. of water molecules	No. density (atoms/Å ³)	Box size (Å)
0.27	298	amb	600	162	438	0.0967	28.69
0.27	298	2.0	600	162	438	0.1142	27.68
0.50	200	amb	600	300	300	0.1027	29.74
0.50	200	2.0	600	300	300	0.1158	28.57
0.50	298	2.0	600	300	300	0.1080	29.24
0.54	298	amb	600	324	276	0.0955	30.73
0.54	190	amb	600	324	276	0.1000	30.26
0.70	298	amb	424	297	127	0.0934	28.50
0.70	298	2.0	424	297	127	0.107	27.22

terms for each atom type. Our previous studies^{4,18} have shown this code and these potentials can predict the local and extended structural and dynamical behavior's of these mixtures across the composition range in close agreement with empirical observation. The simulations were run to produce 2 ns trajectories using 0.5 fs time step with an equilibration time of over 0.5 ns. The sampling interval on the trajectories were every 0.1 ps. Due to this wealth of data, most of the subsequent statistical analysis was done only on the second half of the trajectory giving around 10 000 data points. Details of systems used in simulations are given in Table II.

Temporal averages of the molecular dynamics (MD) simulations and configurational averages of the EPSR-generated ensembles were then interrogated to extract complete sets of intermolecular structural correlations including information on short-range (solvation) and medium-range (clustering) structures. In the case of water, clusters are defined by those molecules that participate in a continuous hydrogen-bonded network. Two water molecules are considered to be hydrogen-bonded if the interoxygen contact distance is less than ≈ 3.5 Å, the radial distance of the first minimum of the $g_{O_w-O_w}(r)$ pair correlation function for both EPSR and MD ensembles. The definition of a cluster is ambiguous in the case of methanol and can be made two different ways. The first is on the basis of hydrogen-bond connectivity, i.e., if constituent methanol oxygen atoms are at a distance less than the first minimum in the $g_{O-O}(r)$ pair correlation function. The second is through methyl group association, where two methanol molecules are assigned to the same cluster if the C-C distance is less than the minimum following the first peak determined from the $g_{O-O}(r)$ pair correlation function (which is ≈ 5.7 Å). The former is more common in pure methanol whereas the latter connectivity type is believed to be characteristic of molecular association that is driven by the hydrophobic interaction. These two types of clusters are subsequently referred to as polar contact clusters and nonpolar contact clusters.

III. RESULTS

A. Cluster distributions at low temperature

We have already demonstrated in a previous publication⁴ that the methanol-water system exhibits significant micro-segregation across a wide range of compositions, forming

localized pockets of a single species of varying size and topology. These clusters are characterized according to the criteria outlined previously. The behavior of water cluster distributions on cooling at mole fraction $x=0.54$ are shown in Fig. 2. The number of clusters containing i molecules is plotted as a fraction of total number of clusters, $M(i)/M$ [where $M=\sum_i M(i)$] against the cluster size i . The cluster distributions show an enhanced probability of the largest clusters on cooling, at the expense of medium-sized (100 molecules or so) clusters. There are slight differences in the experimental and simulation-derived distribution plots; the depleted region of medium-sized clusters in the MD simulations is wider and the enhanced peak of the largest clusters is narrower than the corresponding features in the experimental plot. However, the plots do show the same trends, with the main features being that the system exhibits larger water clusters and these clusters are more frequently present upon cooling. This is consistent with increased segregation of the two components upon cooling. The same trends are seen in the EPSR analysis of a mole fraction $x=0.27$ mixture, although the effect is less marked since the water clusters are already bigger at this concentration. Results of MD simulations at other compositions (not shown) show the same behavior in water cluster size distribution on cooling.

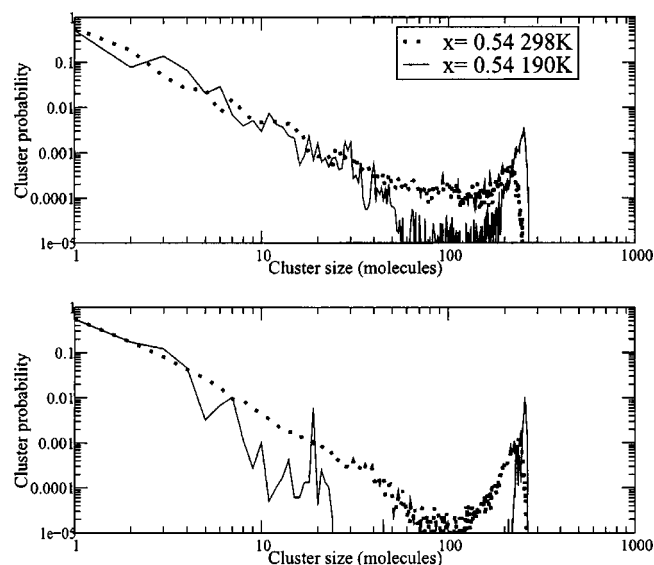


FIG. 2. The effect of cooling on water cluster distributions for $x=0.54$ from EPSR analysis (top) and MD simulations (below).

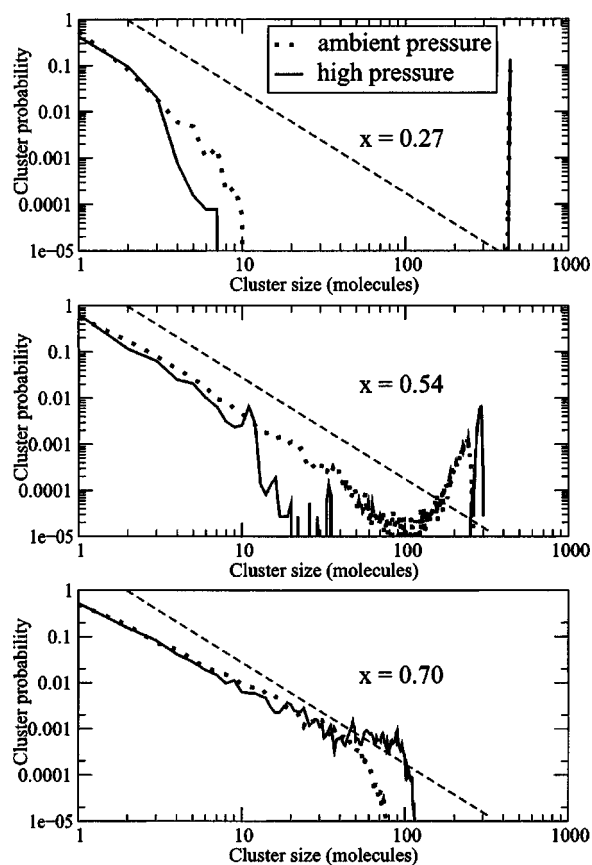


FIG. 3. The effect of compression on MD simulation cluster distributions for mole fraction $x=0.27$ (top), $x=0.54$ (middle), and $x=0.70$ (bottom) for water clusters. Ambient conditions are shown as dotted lines and high pressure shown as solid lines. The predicted power law $n_s \approx s^{-2.2}$ for random percolation on a 3D cubic lattice (Ref. 19) is shown as a dashed line.

B. Cluster distributions at elevated pressure

The effect of compression to 2 kbar on the ambient temperature methanol-water cluster distributions determined by analysis of MD simulations is shown in Fig. 3 at several concentrations, $x=0.70$, $x=0.54$, and $x=0.27$. Also shown is the predicted power law $n_s \approx s^{-2.2}$ for random percolation on a three-dimensional (3D) cubic lattice.¹⁹ The results for water clusters in the system and the effect of increased pressure are most evident on the solutions of methanol mole fraction $x=0.7$ and $x=0.54$. In both cases, the size and probability of occurrence of the largest water clusters are increased. Particularly striking is the case of the most concentrated ($x=0.7$) mixture where compression of 2 kbar changes the water connectivity from isolated nonspanning clusters to a percolating network. The effect on the most dilute solution ($x=0.27$) is less obvious as the ambient pressure results indicate that this solution already comprises very large water clusters, in excess of the theoretical limit for random percolation. We thus find that the effect of pressure is also to enhance segregation at all concentrations studied. The qualitative effect of compression is therefore very surprising, being the same as the effect of cooling. This result is unexpected and contradictory to the general expectation that compression should have had the opposite, destructuring effect. The methanol cluster distributions, both nonpolar and polar (as defined previously), were also explored. In the case

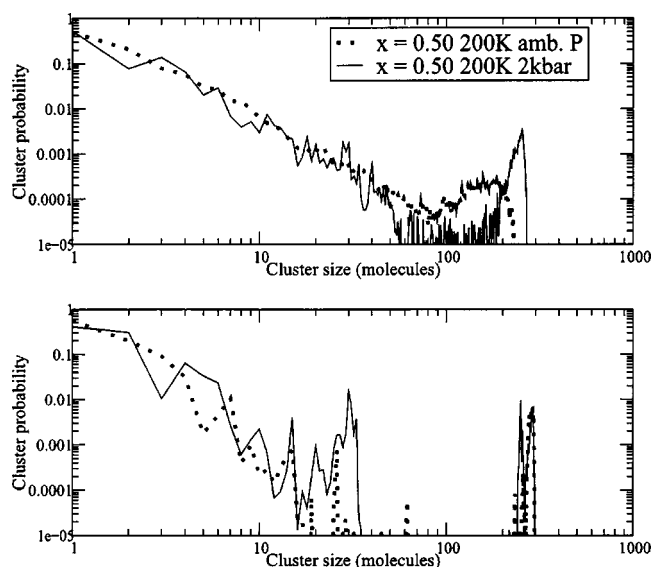


FIG. 4. The effect of compressing a cooled system for mole fraction $x=0.50$ on water cluster distributions from EPSR analysis (top) and MD simulations (below).

of the nonpolar clusters, it is difficult to discern a notable effect of compression: the cluster distributions of even the ambient pressure systems are dominated by large clusters, often comprising all the methanol in the system. Likewise for the polar clusters, of which there are only a relatively small number of small clusters, the effect of compression is rather small.

C. Cluster distributions at elevated pressure and reduced temperature

We also consider the effect of compressing the cooled system. Figure 4 shows the corresponding results for water clusters from EPSR analysis of the neutron data and MD simulations obtained at $x=0.50$ and $T=200$ K at ambient pressure and 2 kbar. The effect of compressing a cooled system appears to be a further enhanced probability of larger water clusters, as was seen previously for the effects of lowered temperature or compression alone. The effect is clearest from the EPSR analysis, where once again the depletion of medium-sized water clusters is evident. The cluster distribution shows an enhanced probability of the largest clusters on compression, at the expense of these medium-sized clusters. The data from the MD simulations are broadly consistent with this picture, and appear to show a bimodal distribution of large cluster sizes, centered around 250 and 280 water molecules. At this composition, there are only 300 water molecules in the system, indicating that these two peaks actually pertain to the same cluster, which absorbs or sheds smaller clusters during the course of the simulation. The prominent peak around a cluster size of 30 is a strong candidate for involvement in this process. We return to the differences between EPSR and MD data in the Discussion.

D. Local structure

In this section we examine the local structure focusing on the pressure and temperature behavior of the water oxy-

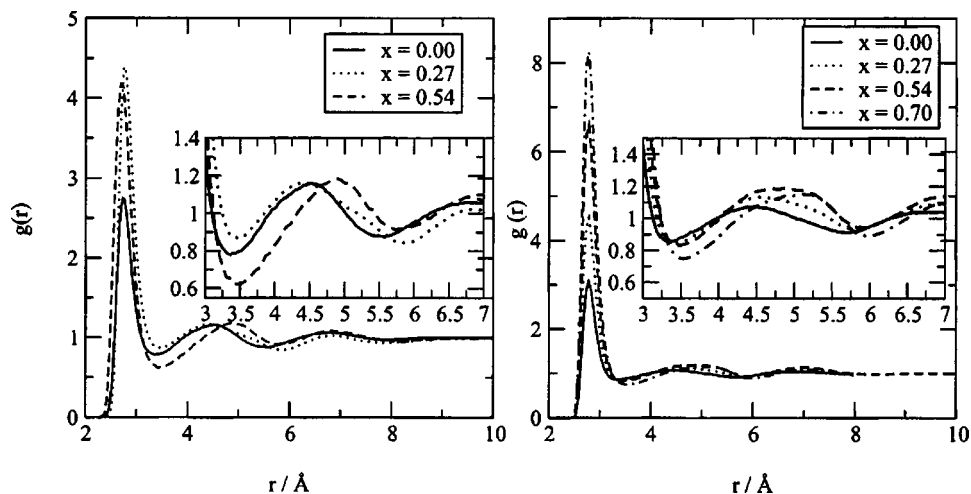


FIG. 5. Water radial distribution functions $g_{O_w-O_w}(r)$ from both EPSR analysis (left) and MD simulations (right) at different concentrations. Inset shows detail of second peak.

gen radial distribution function (RDF) $g_{O_w-O_w}(r)$. We first consider the effects of concentration on this RDF at ambient temperature and pressure. Figure 5 shows data from both EPSR and MD analyses. Even at the lowest concentration, with mole fraction $x=0.27$ we find that a perturbation to $g_{O_w-O_w}(r)$ compared to that of pure water is evident. The location of the second maximum shifts $\approx 0.2 \text{ \AA}$ to higher r from the MD simulations. At increasing concentrations we find, for both experiment and MD simulation, progressively larger shifts in the second peak position to larger r values. This shifts to higher r implies that the water clusters are becoming less like bulk water, which is supported by cluster distribution,⁴ which shows smaller average water cluster sizes with increasing methanol concentration. We assume this is a consequence of the water being confined to increasingly smaller domains by the surrounding methanol hydroxyl groups and consequent interfacial tension.

The effect of cooling on $g_{O_w-O_w}(r)$ is also shown in Fig. 6. At $x=0.27$ (not shown) we find that the main features of the distribution are sharpened, perhaps indicative of reduced dynamic disorder but that there are no other significant

changes. By contrast, at the higher alcohol concentration of $x=0.54$, comparatively large structural perturbations induced by the presence of the alcohol molecules are partially reversed on cooling and the displaced second shell peak in the radial distribution function moves back towards its original position (i.e., of pure water). As the position of this second peak is generally associated with tetrahedrality of the local water structure, both the EPSR analysis of the experimental data and the MD simulations suggest that the previously perturbed tetrahedral structure of the water is recovered on cooling.

We next consider the effect of compression on the local structure at ambient temperature. MD simulations of a $x=0.54$ mole fraction solution do not show any obvious change to the position of the second peak in the $g_{O_w-O_w}(r)$ (in contrast to the data in Fig. 6 for low temperature). Interestingly, it is the methanol $g_{C-C}(r)$ radial distribution function which is perturbed most significantly, and this is shown in Fig. 7. At three different concentrations $x=0.70$, $x=0.54$, and $x=0.27$, the first and second peaks in $g_{C-C}(r)$ are seen to shift to lower r values. This shift is approximately the same

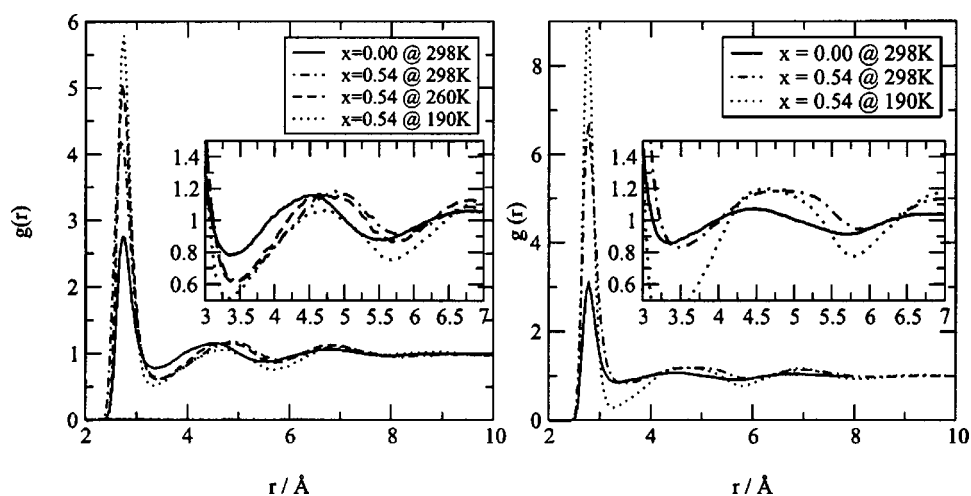


FIG. 6. The effect of cooling on the water radial distribution function $g_{O_w-O_w}(r)$ from both EPSR analysis (left; $x=0.54$ at 298 K, 260 K, and 190 K) and MD simulation (right; $x=0.54$ at 298 K and 190 K).

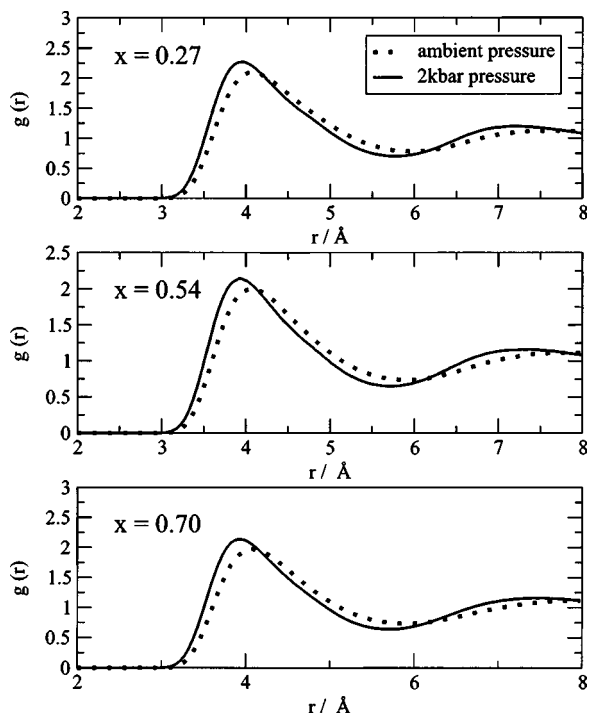


FIG. 7. Methanol $g_{C-C}(r)$ radial distribution functions from MD simulations (mole fraction $x=0.27$, 0.54 , and 0.70).

for all concentrations as the methanol content is increased. This indicates that the methyl groups are squeezed together as the pressure is increased. It appears that it is the methanol which is most responsive to the pressure.

Finally we consider the combined effect of reduced temperature and elevated pressure on the local structure. We might have expected the combined effect to be similar to the sum of the effects of the constituent parts. However, from both EPSR analysis and MD simulations we find (see Fig. 8) that compression of a cooled solution results in a further shift to lower r of the second peak in the $g_{O_w-O_w}(r)$. Thus water appears to partially recover its unperturbed (i.e., ambient pressure and temperature) structure. In addition, the first and second peaks in the methanol $g_{C-C}(r)$ are shifted to lower r , analogous with the situation for the compression of the solution at ambient temperature.

IV. DISCUSSION

The prediction from both the EPSR analysis and MD simulations is one of enhanced segregation of methanol and water on cooling, evidenced by the more frequent existence of larger water clusters, in comparison to room temperature data. This is the kind of behavior we would expect on a microscopic scale if the system were moving towards a phase boundary, characterized by an upper critical solution temperature. Such immiscibility has not been observed in the methanol-water system; this is because the intervening solid phase precludes access to any possible two-fluid region in methanol-water mixtures. The clustering behavior at low temperature provides a consistent framework within which to interpret the observed variations in local structure, particularly $g_{O_w-O_w}(r)$. As the temperature is lowered the formation of larger clusters leads to increased connectivity of the water domains. Within these growing water clusters the local structure evolves toward that of bulk water. The effect is most obvious with the methanol-rich solutions studied, of mole fraction $x=0.54$.

Compression of the solution leads to the same effect on the medium-range order of the system, that is, to enhance segregation by formation of larger water clusters. However, the local structure shows little if any change in the positions of the peaks in $g_{O_w-O_w}(r)$. In contrast, the corresponding RDF for methanol carbon atoms in systems at elevated pressure is displaced to lower r at all concentrations. It would seem therefore that the topology of the larger clusters formed by enhanced pressure is different to those formed by lowered temperature, since the water contained within them does not show a significant trend in the RDF back towards that of bulk water (as was the case for lowered temperature).

Both the MD simulations and the EPSR analysis predict qualitatively the same trends of enhanced clustering as a function of lowered temperature and increased pressure. There are, however, differences in the predicted cluster distributions. These minor differences may be due to the differences in the interatomic potentials used in the EPSR and MD analysis. We have not made a systematic study of the sensitivity of the cluster distributions to interaction potentials. The qualitative trends are clear from both analyses; that cluster-

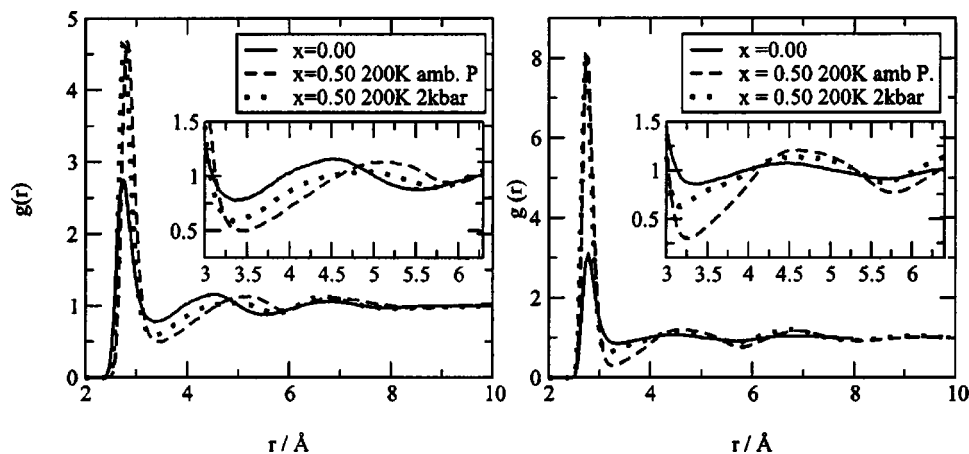


FIG. 8. Water radial distribution functions $g_{O_w-O_w}(r)$ for mole fraction $x=0.50$ at 200 K, variable pressure from EPSR analysis (left) and MD simulations (right).

ing, and hence segregation of the two species, is enhanced by elevated pressure or reduced temperature. A clear example of the differences in distributions is shown in Fig. 4 for the compression of a low temperature $x=0.54$ mole fraction solution. The EPSR analysis clearly shows that the size of the largest water cluster increases and clusters of that size are more frequently found compared to the ambient pressure case. The MD results, on the other hand, are indicative of larger clusters in the sense that they predict the existence of two very large clusters (though not simultaneously) centered around 250 and 280 molecules. The combined probability of these clusters is greater than that of the largest clusters present in the ambient pressure data.

We note that our results concerning the enhanced segregation at elevated pressure are in contrast to the results of Hummer *et al.*²⁰ who have concluded that pressure destabilizes the contact configuration of nonpolar molecular groups, relative to a solvent-separated configuration. These authors then assert that pressure denaturation of proteins proceeds by a similar mechanism, that is solvent penetration into a hydrophobic core. In contrast to this our results from diffraction measurements and simulations indicate the hydrophobic groups get pushed closer together with pressure. This difference may be due to the consequence of having an amphiphile in solution rather than a simple hydrophobe.

V. CONCLUSION

A series of methanol-water solutions have been investigated by neutron diffraction and MD simulation over a range of concentrations, temperatures, and pressures. The diffraction data were analyzed using the EPSR technique which was found to give results qualitatively similar to that from MD simulations, although there are some differences in detail. A general conclusion of these studies is that lowering the temperature has the effect of enhancing the degree of micro-segregation between methanol and water that occurs in these systems.

More surprisingly, increasing the pressure appears to have the same effect, which argues against the notion that pressure denaturation of proteins is caused by water entering the hydrophobic core of a protein: if it did so we might have expected to see a decrease in the clustering with increased pressure, not increased clustering. The second shell of water $g_{O_w-O_w}$ appears to expand slightly with increasing methanol concentration, suggesting a general opening up of the water structure as the water concentration diminishes: this effect is to be analysed to identify whether it is primarily a surface effect or proceeds throughout the water. This expansion is if anything reversed on lowering the temperature or increasing

the pressure. We speculate that these trends could be an indication of the approach to an upper critical solution boundary, which, however, is not observed due to the intervening solid phases.

Overall the methanol-water system has proved itself to be a rich source of phenomena which may be of relevance to situations involving much larger and more complicated molecules. Methanol and water are ideally suited to the experimental diffraction and atomistic simulation methodologies due to their simple molecular forms and their ready availability in different isotopic forms. Yet this simple model system can apparently capture much of the essence of hydrophobicity in aqueous systems in a way that it might occur in the much larger molecular entities, with mixed hydrophobic and hydrophilic headgroups of real biological systems. The present results should therefore help guide the search for possible mechanisms which control molecular conformation in aqueous solution.

ACKNOWLEDGMENTS

The authors acknowledge the technical assistance of John Dreyer, Jonathan Bones, and Chris Goodway at the ISIS Facility, without which the experiments described in this paper would not have been possible. Funding from EPSRC is also gratefully acknowledged.

- ¹S. Dixit, J. Crain, W. Poon, J. Finney, and A. Soper, *Nature (London)* **416**, 829 (2002).
- ²S. Dixit, W. Poon, and J. Crain, *J. Phys.: Condens. Matter* **12**, L323 (2000).
- ³S. Dixit, A. Soper, J. Finney, and J. Crain, *Europhys. Lett.* **59**, 377 (2002).
- ⁴L. Dougan, S. P. Bates, R. Hargreaves, J. P. Fox, J. Crain, J. L. Finney, V. Réat, and A. K. Soper, *J. Chem. Phys.* **121**, 6456 (2004).
- ⁵G. Schneider, *Phys. Chem. Chem. Phys.* **4**, 845 (2002).
- ⁶G. Jackson, *Mol. Phys.* **72**, 1365 (1991).
- ⁷L. Davies, G. Jackson, and L. Rull, *Phys. Rev. Lett.* **82**, 5285 (1999).
- ⁸K. Marsh and F. Kohler, *J. Mol. Liq.* **30**, 13 (1985).
- ⁹P. Postorino, M. A. Ricci, and A. K. Soper, *J. Chem. Phys.* **101**, 4123 (1994).
- ¹⁰A. Soper and A. Luzar, *J. Chem. Phys.* **97**, 1320 (1992).
- ¹¹A. Soper, *Chem. Phys.* **202**, 295 (1996).
- ¹²H. J. C. Berendsen, J. R. Grigera, and T. P. Straatsma, *J. Phys. Chem.* **91**, 6269 (1987).
- ¹³M. Haughney, M. Ferrario, and I. R. MacDonald, *J. Phys. Chem.* **91**, 4934 (1987).
- ¹⁴M. Allen and D. Tildesley, *Computer Simulations of Liquids* (Oxford University Press, Oxford, UK, 1987).
- ¹⁵W. Smith and T. Forester, *J. Mol. Graphics* **14**, 136 (1996).
- ¹⁶J. Pereira, C. Catlow, and G. Price, *J. Phys. Chem. A* **105**, 1909 (2001).
- ¹⁷M. Levitt, M. Hirschberg, R. Sharon, K. Laidig, and V. Daggett, *J. Phys. Chem. B* **101**, 5051 (1997).
- ¹⁸S. Allison, R. Hargreaves, J. Fox, and S. Bates, *Phys. Rev. B* **71**, 024201 (2005).
- ¹⁹N. Jan, *Physica A* **266**, 72 (1999).
- ²⁰G. Hummer, S. Garde, A. García, M. Paulaitis, and L. Pratt, *Proc. Natl. Acad. Sci. U.S.A.* **95**, 1552 (1998).